

Galactic cosmic-ray hydrogen spectra in the 40-300 MeV range measured by the High-energy Particle Detector (HEPD) on board the CSES-01 satellite during the current solar minimum

Matteo Martucci^{1,2,*} on behalf of the LIMADOU-HEPD Collaboration
(a complete list of authors can be found at the end of the proceedings)

¹*INFN - Sezione di Roma "Tor Vergata", V. della Ricerca Scientifica 1, I-00133 Rome, Italy*

²*University of Rome "Tor Vergata", Department of Physics, V. della Ricerca Scientifica 1, I-00133 Rome, Italy*

E-mail: matteo.martucci@roma2.infn.it

The High-Energy Particle Detector (HEPD) onboard the China Seismo-Electromagnetic Satellite (CSES-01) - launched in February 2018 - is a light and compact payload suitable for measuring electrons (3-100 MeV), protons (30-300 MeV), and light nuclei (up to a few hundreds of MeV) with a high energy resolution and a wide angular acceptance. The very good capabilities in particle detection and separation, together with the Sun-synchronous orbit, make HEPD well suited for galactic particles and solar modulation studies. We report here some insights on the data-analysis techniques employed for this kind of study; as a result, semiannual galactic hydrogen differential energy spectra between 40 and 250 MeV for the period between the end of the 24th and the start of the 25th solar activity cycle, are presented. Moreover, a brief discussion on the comparison with theoretical spectra obtained from the HelMod 2D Monte Carlo model is also presented.

37th International Cosmic Ray Conference (ICRC 2021)
July 12th – 23rd, 2021
Online – Berlin, Germany

*Presenter

1. Introduction

Hydrogen nuclei are the most abundant component of charged galactic cosmic rays (GCRs), representing $\sim 90\%$ of the total CR budget. Together with helium nuclei, they account for almost 99% of the entire cosmic radiation. The majority of CRs are believed to be accelerated in supernova remnants (SNRs) in the Galaxy, but all evidence in support of this mechanism is still inferred in an indirect way [1–6]. CRs propagate from their site of production and acceleration through the Milky Way, interacting with the interstellar medium and diffusing on the magnetic field - which permeates space - before reaching the Earth's solar system [7]. These processes modify the CR spectral shape with respect to the acceleration site and in the last 10 years many experiments have found particular features in CR proton and helium nuclei spectra at energies >200 GeV [8, 9]; meanwhile, at much lower energies (below a few GeV), the spectrum is bent downward because of the modulation effect exerted by the turbulent magnetized wind originated from the Sun. Such phenomenon, called solar modulation, is the sum of a series of effects like convection, diffusion, adiabatic deceleration, and drift motions, all driven by the Heliospheric Magnetic Field (HMF) and with a strong time-dependent nature [10, 11]. The portion of the spectrum below a few hundreds MeV is particularly interesting because the modulation effects are stronger and also because this range has been studied mostly by balloons [12–14] and, more recently, by the PAMELA experiment in both the 23^{rd} [15] and 24^{th} solar cycles [16].

In this work - published in 2020 [17] - we present three semi-annual cosmic ray hydrogen spectra measured by the High-Energy Particle Detector in the ~ 40 MeV-250 MeV range, during the period between the very end of the 24^{th} solar cycle and the beginning of the 25^{th} - from August 2018 to January 2020.

2. The HEPD detector and CSES Mission

The High-Energy Particle Detector (HEPD) is a light and compact (40.36 cm \times 53.00 cm \times 38.15 cm, total mass ~ 45 kg) payload designed and built by the Limadou Collaboration, the Italian branch of the CSES mission. From top to bottom, the apparatus consists of a tracking system, including two 213.2 mm \times 214.8 mm \times 0.3 mm double-sided silicon microstrip planes, followed by a trigger system consisting of one EJ-200 plastic scintillator layer segmented into six paddles (20 cm \times 3 cm \times 0.5 cm each) and readout by two Photomultiplier Tubes (PMTs). The central portion of the instrument is occupied by a range calorimeter composed of two sections. The upper part, called TOWER, is a stack of 16 EJ-200 plastic scintillator planes (15 cm \times 15 cm \times 1 cm), each one read out by two PMTs. The lower part is a 3×3 matrix of LYSO (Lutetium-Yttrium Oxyorthosilicate) inorganic scintillator crystals, 5 cm \times 5 cm \times 4 cm each; each crystal is read out by a single PMT. Finally, an anti-coincidence (VETO) system embeds the entire instrument and is composed of five EJ-200 plastic scintillator planes (0.5 -cm thick), each one read out by two PMTs; four planes out of five surround the detector laterally, and one is placed below the LYSO matrix. The payload has a $\pm 60^\circ$ Field-of-View and a Geometrical Acceptance of more than 400 cm²sr @90 MeV for protons. A more detailed description of the instrument can be found in [18, 19].

HEPD was launched on board the China Seismo-Electromagnetic Satellite (CSES) [20] on February 2, 2018 in the framework of a mission designed to investigate the top side of the ionosphere and to

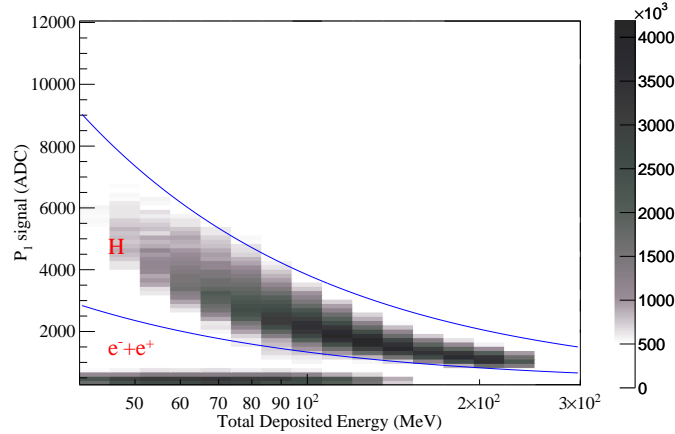


Figure 1: The P_1 signal distribution as a function of the total energy lost in the detector; the blue curves represent the 15% and 95% quantile threshold used to select the hydrogen band.

gather data on the near-Earth electromagnetic and particle environment with special focus on the lithosphere-atmosphere-ionosphere coupling. The satellite was put into a Sun-synchronous orbit, at ~ 507 km altitude, 97° inclination and with a revisit time of ~ 5 days. Due to attitude adjustments and other programmed maneuvers, HEPD (together with the other payloads on board CSES-01) is switched off below -65° and above $+65^\circ$, but thanks to the large detector aperture, HEPD is able to collect galactic particles, even if for a small amount of time per day.

3. Data Analysis

In order to give a valid trigger to start data acquisition and to avoid multi-particle events and reduce secondaries generated in the upper portion of the payload (TOWER), a particle must cross a single paddle of the trigger plane and at least the first two planes of the TOWER, P_1 and P_2 . After that, only particles fully contained (i.e. those that stop inside the TOWER+LYSO sub-detector) are included in the final flux sample, therefore discarding particles generating signal in one of the VETO planes. This is mandatory to guarantee that the entire energy of the primary particle is deposited inside the detector. To discriminate between hydrogen nuclei and electrons/positrons populations, a double-curve selection on the signal deposited on the first scintillator plane (P_1) as a function of the total deposited energy, is required. The P_1 signal distribution as a function of the energy lost in the TOWER+LYSO sub-detector, is shown in Figure 1; the blue curves represent the 15% and 95% quantile threshold used to select the hydrogen band.

The highly inclined orbit of the CSES-01 satellite allows particles of various origin to be detected. To separate the primary (solar or galactic) component from the re-entrant albedo component, it is necessary to evaluate the local rigidity cutoff (R) in each point of the orbit. Due to the large acceptance of HEPD, the Störmer approximation of vertical approaching particles is no longer valid; for this reason, a simulation on all possible arrival directions of protons has been carried out, considering the instrument Field-of-View (FoV). A combination of the International Geomagnetic Field Reference (IGRF) model [21] and Tsyganenko89 model [22] is adopted to take

into consideration both internal and external magnetic field sources. As a result, a latitude/longitude static cutoff map is obtained and employed as a template for the analysis.

For consistency with the aforementioned geographical selection criteria, the live time τ_{live} calculation of the apparatus - performed and managed via the trigger board - is accumulated only in polar regions, where the rigidity cutoff is $0.26 \text{ GV} < R < 0.35 \text{ GV}$.

The geometrical factor of HEPD is defined by the requirement of containment within the volume of the instrument: an incoming particle entering the upmost section of the payload, must be fully contained inside the calorimeter (TOWER+LYSO). It is evaluated using a Monte Carlo simulation of isotropically generated ($0^\circ < \theta < 90^\circ$ and $0^\circ < \phi < 180^\circ$) protons with primary energy ranging from 1 MeV to 10 GeV. A careful digitization procedure, aimed to introduce instrumental ADC signal response in the simulation itself, is designed to reproduce and match the in-flight conditions. Selection efficiencies include both particle selection and instrumental efficiency. The former refers to the double-curve selection as a function of deposited energy, depicted in Figure 1. The resulting efficiency is $\sim 78\%$, almost constant between 40 and 250 MeV, and it is estimated using the digitized Monte Carlo simulation already described. On the other hand, the latter comprises all the instrumental inefficiencies that cannot be estimated by only using simulations, such as the variation in the response of sensitive components, aging processes and so on.

The major source of contamination for the low-energy hydrogen sample is given by $>40 \text{ MeV}$ electrons. Usually these MIP-like particles deposit a small amount of energy in the scintillators, being consequently rejected by the double-curve selection displayed in Figure 1; however, if they impinge the detector with an inclined trajectory, their energy release could be greater, thus contaminating the sample. To remove this effect, a dedicated simulation is carried out.

Finally, the proton energy spectrum measured in the entire calorimeter is corrected to account for particle slow-down and energy loss in the trigger paddles, tracker planes and various passive structures. The correction is applied by means of an unfolding procedure, following the classical Bayesian approach of [23]. A complete description of the analysis can be found in [17].

4. Results

Three semi-annual galactic hydrogen spectra as a function of energy between 40 and 250 MeV have been obtained in three different consecutive time periods (from August 6, 2018 to January 5, 2020) very much inside the heliosphere (1 AU); the energy profiles are shown as black circles in Figure 2, compared to the theoretical prediction from the HelMod model [24] in the same period. As a further comparison, data from the SOHO/EPHIN spacecraft (red square marker) between 40 MeV and 53 MeV are also presented [25]. The agreement seems to be good in all the three examined periods, considering both statistical and systematic uncertainties. A more detailed discussion on these results can be found in [17] and during the presentation, together with some new results on solar modulation.

References

- [1] M. Ackermann, M. Ajello, A. Allafort, L. Baldini, J. Ballet, G. Barbiellini et al., *Detection of the Characteristic Pion-Decay Signature in Supernova Remnants*, *Science* **339** (2013) 807

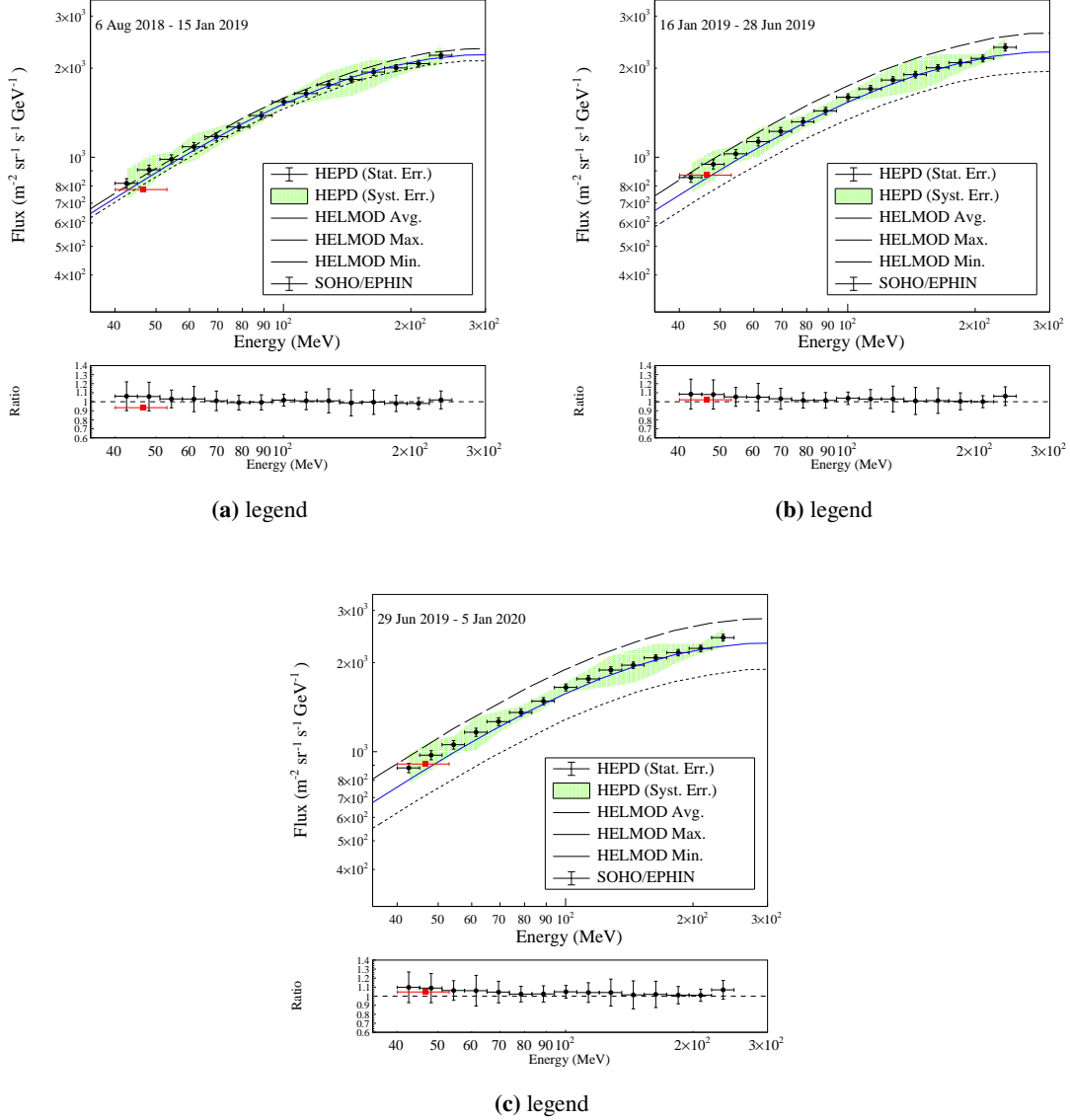


Figure 2: Large panel: galactic proton spectra as a function of energy measured by HEPD in the three intervals described in the text - from August 6, 2018 to January 15, 2019 (a), from January 16, 2019 to June 28, 2019 (b) and from June 29, 2019 to January 5, 2020 (c), respectively. Systematic uncertainties are also present as a green shaded area. The continuous curves represent, respectively, the HelMod theoretical spectrum averaged over the period under study (blue solid line), the maximum (dashed line) and minimum (dotted line) expected deviation from the model itself. The red square represents data obtained from SOHO/EPHIN spacecraft. Narrow panel: ratio between HEPD data and HelMod model, as a function of energy; errors on HEPD data are a sum of statistical and systematic uncertainties.

- [1302.3307].
- [2] M. Tavani, A. Giuliani, A.W. Chen, A. Argan, G. Barbiellini, A. Bulgarelli et al., *Direct Evidence for Hadronic Cosmic-Ray Acceleration in the Supernova Remnant IC 443*, *Astrophys. J. Lett.* **710** (2010) L151 [1001.5150].
- [3] F. Giordano, M. Naumann-Godo, J. Ballet, K. Bechtol, S. Funk, J. Lande et al., *Fermi Large Area Telescope Detection of the Young Supernova Remnant Tycho*, *Astrophys. J. Lett.* **744** (2012) L2 [1108.0265].
- [4] V.A. Acciari, E. Aliu, T. Arlen, T. Aune, M. Beilicke, W. Benbow et al., *Discovery of TeV Gamma-ray Emission from Tycho's Supernova Remnant*, *Astrophys. J. Lett.* **730** (2011) L20 [1102.3871].
- [5] E.G. Berezhko and H.J. Völk, *Spectrum of Cosmic Rays Produced in Supernova Remnants*, *Astrophys. J. Lett.* **661** (2007) L175 [0704.1715].
- [6] J. Vink, *Supernova remnants: the X-ray perspective*, *Astron. Astrophys. Rev.* **20** (2012) 49 [1112.0576].
- [7] E. Amato and P. Blasi, *Cosmic ray transport in the galaxy: A review*, *Advances in Space Research* **62** (2018) 2731 .
- [8] O. Adriani, G.C. Barbarino, G.A. Bazilevskaya, R. Bellotti, M. Boezio, E.A. Bogomolov et al., *PAMELA Measurements of Cosmic-Ray Proton and Helium Spectra*, *Science* **332** (2011) 69 [1103.4055].
- [9] AMS COLLABORATION collaboration, *Precision measurement of the proton flux in primary cosmic rays from rigidity 1 GV to 1.8 TV with the alpha magnetic spectrometer on the international space station*, *Phys. Rev. Lett.* **114** (2015) 171103.
- [10] M.S. Potgieter, *Cosmic Rays in the Inner Heliosphere: Insights from Observations, Theory and Models*, *Space Sci. Rev.* **176** (2013) 165.
- [11] M. Potgieter, *The global modulation of cosmic rays during a quiet heliosphere: A modeling perspective*, *Advances in Space Research* **60** (2017) 848 .
- [12] P.S. Freier and C.J. Waddington, *Singly and doubly charged particles in the primary cosmic radiation*, *J. Geophys. Res.* **73** (1968) 4261.
- [13] G.D. Badhwar, C.L. Deney, B.R. Dennis and M.F. Kaplon, *Measurements of the Low-Energy Cosmic Radiation during the Summer of 1966*, *Physical Review* **163** (1967) 1327.
- [14] T.L. Garrard, E.C. Stone and R.E. Vogt, *Solar Modulation of Cosmic-Ray Protons and He Nuclei*, in *International Cosmic Ray Conference*, vol. 2 of *International Cosmic Ray Conference*, p. 732, Jan., 1973.

- [15] O. Adriani, G.C. Barbarino, G.A. Bazilevskaya, R. Bellotti, M. Boezio, E.A. Bogomolov et al., *Time Dependence of the Proton Flux Measured by PAMELA during the 2006 July-2009 December Solar Minimum*, *Astrophys. J.* **765** (2013) 91 [1301.4108].
- [16] M. Martucci, R. Munini, M. Boezio, V. Di Felice, O. Adriani, G.C. Barbarino et al., *Proton Fluxes Measured by the PAMELA Experiment from the Minimum to the Maximum Solar Activity for Solar Cycle 24*, *Astrophys. J. Lett.* **854** (2018) L2 [1801.07112].
- [17] S. Bartocci, R. Battiston, W.J. Burger, D. Campana, L. Carfora, G. Castellini et al., *Galactic cosmic-ray hydrogen spectra in the 40–250 MeV range measured by the high-energy particle detector (HEPD) on board the CSES-01 satellite between 2018 and 2020*, *The Astrophysical Journal* **901** (2020) 8.
- [18] A. Ambrosi and et al., *The HEPD particle detector of the CSES satellite mission for investigating seismo-associated perturbations of the Van Allen belts*, *Science China Technological Sciences* **61** (2018) 643.
- [19] P. Picozza, R. Battiston, G. Ambrosi, S. Bartocci, L. Basara, W.J. Burger et al., *Scientific Goals and In-orbit Performance of the High-energy Particle Detector on Board the CSES*, *Astrophys. J. Suppl.* **243** (2019) 16.
- [20] X. Shen and et al., *The state-of-the-art of the China Seismo-Electromagnetic Satellite mission*, *Science China Technological Sciences* **61** (2018) 634.
- [21] E. Thébault, C.C. Finlay, C.D. Beggan, P. Alken, J. Aubert, O. Barrois et al., *International Geomagnetic Reference Field: the 12th generation*, *Earth, Planets, and Space* **67** (2015) 79.
- [22] N.A. Tsyganenko, *A magnetospheric magnetic field model with a warped tail current sheet*, *Planet. Space Sci.* **37** (1989) 5.
- [23] G. D’Agostini, *Improved iterative Bayesian unfolding*, *arXiv e-prints* (2010) arXiv:1010.0632 [1010.0632].
- [24] M.J. Boschini, S. Della Torre, M. Gervasi, G. La Vacca and P.G. Rancoita, *The HELMOD model in the works for inner and outer heliosphere: From AMS to Voyager probes observations*, *Advances in Space Research* **64** (2019) 2459.
- [25] R. Müller-Mellin, H. Kunow, V. Fleißner, E. Pehlke, E. Rode, N. Röschmann et al., *COSTEP - Comprehensive Suprathermal and Energetic Particle Analyser*, *Sol. Phys.* **162** (1995) 483.

Full Authors List: LIMADOU-HEPD Collaboration

S. Bartocci¹, R. Battiston^{2,3}, F. Benotto⁴, S. Beolè^{4,5}, W.J. Burger^{3,6}, D. Campana⁷, G. Castellini⁸, P. Cipollone¹, S. Coli⁴, L. Conti^{1,9}, A. Contin^{10,11}, M. Cristoforetti¹², L. De Cilladi^{4,5}, C. De Donato¹, C. De Santis¹, F.M. Follega^{2,3}, G. Gebbia^{2,3}, R. Iuppa^{2,3}, M. Lolli¹¹, N. Marcelli^{1,13}, M. Martucci^{1,13}, G. Masciantonio¹, M. Mergé^{1,†}, M. Mese^{7,14}, C. Neubuser³, F. Nozzoli³, A. Oliva¹¹, G. Osteria⁷, L. Pacini¹⁵, F. Palma^{1,†}, F. Palmonari^{10,11}, A. Parmentier¹, F. Perfetto⁷, P. Picozza^{1,13}, M. Piersanti¹⁶, M. Pozzato¹¹, E. Ricci^{2,3}, M. Ricci¹⁷, S.B. Ricciarini⁸, Z. Sahnoun¹¹, V. Scotti^{7,14}, A. Sotgiu^{1,13}, R. Sparvoli^{1,13}, V. Vitale¹, S. Zoffoli¹⁸ and P. Zuccon^{2,3}

¹ INFN-Sezione di Roma “Tor Vergata”, V. della Ricerca Scientifica 1, I-00133 Rome, Italy;

² University of Trento, V. Sommarive 14, I-38123 Povo (Trento), Italy;

³ INFN-TIFPA, V. Sommarive 14, I-38123 Povo (Trento), Italy;

⁴ INFN-Sezione di Torino, Via P. Giuria 1, I-10125 Torino, Italy;

⁵ University of Torino, Via P. Giuria 1, I-10125 Torino, Italy;

⁶ Centro Fermi, V. Panisperna 89a, I-00184 Rome, Italy;

⁷ INFN-Sezione di Napoli, V. Cintia, I-80126 Naples, Italy;

⁸ IFAC-CNR, V. Madonna del Piano 10, I-50019 Sesto Fiorentino (Florence), Italy;

⁹ Uninettuno University, C.so V. Emanuele II 39, I-00186 Rome, Italy;

¹⁰ University of Bologna, V.le C. Berti Pichat 6/2, I-40127 Bologna, Italy;

¹¹ INFN-Sezione di Bologna, V.le C. Berti Pichat 6/2, I-40127 Bologna, Italy;

¹² Fondazione Bruno Kessler, V. Sommarive 18, I-38123 Povo (Trento), Italy;

¹³ University of Rome “Tor Vergata”, V. della Ricerca Scientifica 1, I-00133 Rome, Italy;

¹⁴ University of Naples “Federico II”, V. Cintia 21, I-80126 Naples, Italy;

¹⁵ INFN-Sezione di Firenze, V. Sansone 1, I-50019 Sesto Fiorentino (Florence), Italy;

¹⁶ INAF-IAPS, V. Fosso del Cavaliere 100, I-00133 Rome, Italy;

¹⁷ INFN-LNF, V. E. Fermi 54, I-00044 Frascati (Rome), Italy;

¹⁸ Italian Space Agency, V. del Politecnico, I-00133 Rome, Italy;

† At ASI Space Science Data Center (SSDC) also, V. del Politecnico, I-00133 Rome, Italy.